Bacterial growth laws reflect the evolutionary importance of energy efficiency

Arijit Maitra[1] and Ken A. Dill[1]

Laufer Center for Physical and Quantitative Biology and the Departments of Chemistry and Physics, Stony Brook University, Stony Brook, NY 11794

We are interested in the balance of energy and protein synthesis in bacterial growth. How has evolution optimized this balance? We describe an analytical model that leverages extensive literature data on growth laws to infer the underlying fitness landscape and to draw inferences about what evolution has optimized in *Escherichia coli*. Is *E. coli* optimized for growth speed, energy efficiency, or some other property? Experimental data show that at its replication speed limit, *E. coli* produces about four mass equivalents of nonribosomal proteins for every mass equivalent of ribosomes. This ratio can be explained if the cell's fitness function is the the energy efficiency of cells under fast growth conditions, indicating a tradeoff between the high energy costs of ribosomes under fast growth and the high energy costs of turning over nonribosomal proteins under slow growth. This model gives insight into some of the complex nonlinear relationships between energy utilization and ribosomal and nonribosomal production as a function of cell growth conditions.

growth laws | fitness landscape | energy efficiency | yield | bacterial metabolism

Since the work of Monod in the 1940s, there has been interest in understanding the principles of bacterial growth laws (1–12). Monod observed that increasing glucose increases *Escherichia coli's* growth rate, up to a maximum rate beyond which the cells cannot replicate any faster (1). On the one hand, such growth laws are experimentally observable. On the other hand, growth laws, per se, do not give insight into the evolutionary driving forces that lead to them.

Evolutionary principles are expressed by fitness landscapes (13), which are mathematical surfaces that represent how the organism's fitness depends on some cellular property that can be altered by evolution over time. Peaks on fitness landscapes represent states of maximal fitness. To understand why a cell has a particular growth law, we need a mathematical model that relates its growth law (how the growth rate of the cellular population depends on food concentration) to its underlying fitness landscape (how the cell's growth parameters can be altered through evolution). Thus far, this is relatively uncharted territory for cellular modeling. Here, we develop a model to explore how bacteria balance their fluxes of energy and ribosomal (RPs) and nonribosomal proteins (NRPs). By comparing the model with data, we can explore possible fitness objectives for bacterial replication. Are bacteria evolutionarily optimized to maximize their duplication speed? Or, are bacteria evolutionarily optimized to maximize the energy efficiency of their duplication processes? Or, something else? By "evolutionarily optimized," we mean the tradeoffs that a cell must make. By evaluating extensive growth data on *E. coli* through the lens of the present model, which relates growth observables to fitness landscapes, we conclude that a principal evolutionary driving force for bacteria is the energy efficiency of the fastest-growing cells.

Modeling *E. coli*'s Balance of Energy Flux and Protein Synthesis

Fig. 1 shows our kinetic model of bacteria growing in the exponential phase. This model defines relationships among four dynamical quantities: the rate of synthesis of ribosomal proteins, the synthesis and degradation rates of NRPs, the production and utilization rates of energy (ATP), and the steady-state specific growth rate of the cell. After Scott et al., Klumpp et al., and others (10, 14, 15), we develop a coarse-grained model based on the following observations: (*i*) half of the biomolecular mass in a cell are proteins (16); (*ii*) under fast growth, ~86% of the total RNA investment of a cell is in ribosomes (6); (*iii*) under fast-growth conditions, more than 80% of the cell's ATP requirements for biomass is spent on protein and rRNA synthesis (17, 18); and (*iv*) bacterial fitness costs, defined as relative loss of fitness, increase with excess production of protein (19, 20). Hence our coarse-grained modeling here focuses on just three internal cell components: ATP (our surrogate quantity that represents internal energy supplies, taken broadly), ribosomes (R), and nonribosomal protein (P).*

We model the concentration dynamics as follows:

$$\frac{dR}{dt} = J_r - \lambda R, \qquad [1]$$

$$\frac{dP}{dt} = J_p - (\lambda + \gamma)P, \qquad [2]$$

$$\frac{dA}{dt} = m_a J_a - m_r J_r - m_p J_p - \lambda A, \qquad [3]$$

$$\rho = M_r R + M_p P. \qquad [4]$$

Here, R, P, and A are the concentrations of ribosomes, NRPs, and ATP, respectively, and λ is the specific growth rate of cells. m_a is the stoichiometric number of ATP molecules derived by the cell per glucose molecule, and m_r and m_p are the stoichiometric numbers of ATP molecules required to synthesize a ribosome (i.e., ribosomal
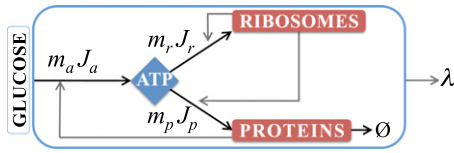
Fig. 1. Minimal model of *E. coli*. Extracellular sugar is converted to ATP, which powers a two-compartment proteome: RPs and NRPs. In turn, the proteome catalyzes the energy-conversion process and growth of the cell. The black arrows show the ATP fluxes: $m_a J_a$ is the influx of sugar conversion to ATP, $m_r J_r$ is the flow of ATP to produce ribosomes, $m_p J_p$ is the flow of ATP to produce NRPs, $\rightarrow \varnothing$ indicates the degradation of NRPs, and λ is the specific growth rate of *E. coli*.

proteins plus ribosomal RNAs) and an NRP, respectively. M_r is the sum of molecular weights of all of the RPs in a ribosome, and M_p is the average molecular weight of an NRP. γ denotes degradation rate of the NRPs (22–24),[†] whereas ribosomes are assumed to be stable (25). The total protein density of a cell is denoted by ρ, and it is conserved over a range of growth rates as observed in experiments. For specific values, see Table 1. The rate equations (Eqs. **1–3**) contain dilution terms (λR), (λP), and (λA), respectively. As the cell grows, its volume increases, so even if the numbers of cellular protein molecules were fixed, their concentrations would diminish as the cell grows. We set $\lambda A = 0$, because this term is negligible compared with the other fluxes in Eq. **3**.[‡]

Now, we express the production–rate fluxes J_r of ribosomal proteins, J_p of NRPs, and the consumption–rate flux of glucose, J_a, for ATP generation in Eqs. **1–3** in terms of concentrations, R, P, A, and extracellular glucose, G

$$J_r = k_r f_r [A(G)] \cdot R, \qquad [5]$$

$$J_p = k_p f_p [A(G)] \cdot R, \qquad [6]$$

$$J_a = k_a(G) \cdot P, \qquad [7]$$

where k_a, k_p, and k_r are rate coefficients. These functions are given explicitly in Eqs. **S1–S5** and Fig. S1*A*. We note here for example that $f_r(A)$ is a step-like activation function that saturates with ATP concentration (which, in turn, depends on glucose) to f_r^∞, whereas $f_p(A) = f_p^\infty$ is nearly independent with cell's energy status (26). We express these functional dependences explicitly above to indicate that even though this coarse-grained model is simple in having few equations, it retains considerable complexity of the nonlinearities and feedback that are essential for treating cells beyond common linear approximations.

Our interest here is in the cell growth dynamics over a time-scale of hours, so we now focus on steady-state conditions. We obtain the three steady-state relationships from this model by setting the time derivatives in Eqs. **1–3** to zero, giving

$$\frac{R}{P} = (\lambda + \gamma)/k_p f_p, \qquad [8]$$

$$\lambda = k_r f_r, \qquad [9]$$

[†]Average cost of making 1 aa is ~2 ATP; average cost of making a peptide bond is ~4 ATP and adding these together gives ~6 ATP. The average cost of making an average RNA nucleotide and joining a pair of nucleotides is ~10 ATP (ref. 16, table 1, chapter 4).

[‡]The justification for $\lambda A \ll (m_r J_r + m_p J_p)$ in Eq. 3 is as follows. From Fig. 2*B*, range of growth rates is 0–1 h^{-1}, whereas the range of ATP concentration is 0.1–10 mM. Therefore, λA varies between 0 and 10 mM/h. Conversely, from Fig. 4*F*, the range of $(m_r J_r + m_p J_p)$ is about 500–15,000 mM/h. These numbers justify $\lambda A \ll (m_r J_r + m_p J_p)$.

$$m_a J_a = m_r J_r + m_p J_p. \qquad [10]$$

Eq. **9** shows that the maximum growth rate of the cell, the "speed limit," is the product (also see ref. 10)

$$\lambda^\infty = k_r f_r^\infty, \qquad [11]$$

of model quantities that depend on how fast ribosomes are made.

Deriving Monod's Growth Law from the Underlying Fitness Landscape

Using this simple coarse-grained model, we develop the central result of this work, namely a mathematical relationship between a growth law (how the growth rate of an average cell depends on food concentration, on timescales shorter than its lifetime) and its fitness landscape (the fitness costs to a cell lineage from altering its machine properties and growth parameters through evolutionary changes on long timescales). We seek an expression for the cell's growth rate $\lambda \equiv \lambda(G, \mathbf{c_m})$, as a function of G, the extracellular sugar concentration, and $\mathbf{c_m}$, the vector of biophysical machine-property set points, such as the degradation and elongation rates of NRPs and maximum rate of ribosomal synthesis. If we had a mathematical function $\lambda \equiv \lambda(G, \mathbf{c_m})$, then varying G at fixed $\mathbf{c_m}$ would express the growth law: how the concentrations and fluxes of A, R, and P depend on sugar as a cell grows. Alternatively, the dependence of λ on $\mathbf{c_m}$ expresses the fitness landscape, namely how the cellular growth rate depends on the cell's intrinsic biochemical and biophysical properties, which have been established through evolution.

To find this function, we solve the set of equations above in the steady-state limit. That leads us to an expression for the growth rate as a cubic polynomial (*SI Text*)

$$a_3 \lambda^3 + a_2 \lambda^2 + a_1 \lambda + a_0 = 0. \qquad [12]$$

where the coefficients a_0, a_1, a_2, and a_3 depend on the glucose concentration, biophysical constants (Table 1), and metabolic parameters (Table 2). Its solution gives $\lambda = \lambda(G, \mathbf{c_m})$, providing both the Monod's growth law and the evolutionary fitness landscape of the model.

Here is how we use this model. First, we use experimental data to determine the parameters of the model (Fig. 2). In particular, we require three types of experimental data: (*i*) the growth rate vs. sugar, $\lambda = \lambda(G)$, such as in Monod's growth law; (*ii*) the ribosomal fraction vs. growth rate, $\phi = \phi(\lambda)$; and (*iii*) the ATP concentration as a function of growth rate, $A = A(\lambda)$. These three types of experiments fully specify the model (*SI Text*). We are especially interested in the energy-mass balance topology and the principles and limits arising out of it over evolutionary timescales. Then, given the fully specified model, we can explore the fitness landscape. In particular, we ask what *E. coli* is optimized to do, in the context of how its energy is trafficked between RPs and NRPs.

Cells Are Optimized for Energy Efficiency of the Fast-Growing Cells and Not Just Growth Rate or Efficiency Alone

We are interested in the cell's energy efficiency. We define the energy efficiency as the growth rate λ divided by the rate, J_a, of conversion of sugar to ATP, specifically

$$\varepsilon(\lambda, f_p^\infty) = \left(\frac{\rho}{m_a}\right)\left(\frac{\lambda}{J_a}\right), \qquad [13]$$

(27). ε is a measure of how effectively the organism converts its input energy into its duplication speed. The energy efficiency ε is a function of the values of the machine constants that have resulted from evolutionary optimization (18, 28, 29).

Table 1. Structural, rate, and bioenergetic constants

Constants	Symbol	Value	Reference
Physical constants			
Protein density	ρ	0.25 g·cm^{-3}	(46)
Molecular weight of RPs per ribosome	M_r	7,336 aa × 110 g/mol/aa = 806,960 g·mol^{-1}	(6)
Molecular weight of an NRP	M_p	325 aa × 110 g/mol/aa = 35,750 g·mol^{-1}	(47)
Molecules of ATP produced per glucose molecule	m_a	30	(32)
Molecules ATP consumed to create one ribosome	m_r	(7,336 aa × 6) + (4,566 nu × 10) ∼ 89,700	[†]
Molecules of ATP consumed to create one NRP	m_p	325 aa × 6 = 1,950	
Rate of NRP elongation per ribosome, 20 aa/s	k_p'	20 × 3,600 (aa/h)/7,336 aa ∼ 10 aa/h/(RP aa)	(6)
Nonribosomal protein degradation rate	γ	0.1 NRP per total NRP per hour	(22)
Derived constants			
Maximum number of protein molecules translated per hour per ribosome (capacity)	k_p	$M_r k_p'/M_p$ = 215 h^{-1}	
NRP translation rate per ribosome scaled by pathway efficiencies	λ_p	$(\varepsilon_r/\varepsilon_p)k_p' \sim$ 5 h^{-1}	
Maximum number of ribosomes synthesized per hour per ribosome ($=\lambda_p$)	k_r	5 h^{-1}	
Ribosomal pathway efficiency, grams of RPs synthesized per mole ATP	ε_r	$M_r/m_r \sim$ 9 g·mol^{-1}	
Protein pathway efficiency, grams of NRPs per mole ATP	ε_p	$M_p/m_p \sim$ 18 g·mol^{-1}	
Relative pathway efficiency between P and R pathways	ε_{rp}	$(\varepsilon_p - \varepsilon_r)/\varepsilon_r \sim$ 1	

[†]Average cost of making 1 aa is ∼2 ATP; average cost of making a peptide bond is ∼4 ATP and adding these together gives ∼6 ATP. The average cost of making an average RNA nucleotide and joining a pair of nucelotides is ∼10 ATP (ref. 16, table 1, chapter 4).

The present model can be used to explore what values of the biophysical constants are optimal. We can compute its point of maximum fitness to address how *E. coli* chooses one of its important operating parameters. Here, we focus on one particular biophysical constant. We suppose some properties are largely fixed by chemical and physical limits, including the rate constants of protein synthesis (k_p'), degradation (γ), and ribosomal assembly (k_r), and the relative costs of P vs. R ($\varepsilon_p/\varepsilon_r$).[§] We suppose that evolution can optimize a cell's ribosome utilization by altering the value of f_p^∞, the fraction of ribosomes that are producing NRPs under fast-replication conditions ($\lambda \to \lambda^\infty$). We ask what value, $f_p^\infty = f_p^{\infty,*}$, maximizes the cell's energy efficiency ε? In *SI Text*, we show that the value of $f_p^{\infty,*}$ that maximizes the energy efficiency of the cell under the fast-growth condition is

$$f_p^{\infty,*} \approx 1 - \frac{1}{k_r}\frac{\gamma}{\varepsilon_{rp}}\left(1 - \frac{k_p'}{k_r}\right) - \frac{1}{k_r}\sqrt{\frac{\gamma}{\varepsilon_{rp}}\,k_p'}. \qquad \textbf{[14]}$$

Substituting the known machine constants from Table 1 into Eq. **14** gives the value $f_p^{\infty,*} \sim 0.8$ and therefore $f_r^{\infty,*} = 1 - f_p^{\infty,*} \sim 0.2$. This result is quite robust, independent of the substrates for growth and the mode of energy metabolism, e.g., fermentation vs. oxidative phosphorylation. A key uncertainty is in ϵ_r. If we increase ϵ_r by 50%, then the model predicts the peak at $f_p^{\infty,*} = 0.69$, which is within the error of the experimental data. This result predicts that, at its maximum speed, each ribosome produces about four mass units of NRP for every mass unit of ribosome it produces. Remarkably, these predicted values are very close to the observed values of f_p for fast-growing aerobic *E. coli* under different conditions (Fig. 3 and Fig. S2*A*).

Here is our interpretation. Consider two idealized limiting cases: (*i*) if a bacterial cell had only one ribosome ($f_p^{\infty,*} \to 1$), the cell would require years to duplicate; or (*ii*) if a bacterial cell was a "bag of ribosomes" ($f_p^{\infty,*} \to 0$), the cell could duplicate in about 6 min. In reality, the observed speed limit for duplicating *E. coli* is about 20–30 min. Therefore, to first approximation, *E. coli* has evolved to nearly reach the bag of ribosomes limit under fast-growth conditions. However, to second approximation, this is not

exactly true. Why is *E. coli* not able to squeeze out the remaining factor of 3–4 in speed? Why must each ribosome duplicate about four times its own weight in NRPs at the cell's speed limit? On the one hand, there could be biological reasons why there is a minimal essential set of NRPs that must be duplicated. On the other hand, we simply note that it is remarkable that the observed mass ratio of four can be derived from a simple principled general energy-balance argument.

Put metaphorically, this evolutionarily optimized energy balance in *E. coli* is akin to optimizing a race car. A race car has a front end (fuel system) and back end (engine). The best race car is one in which the fuel system is matched to the engine, neither too big for the engine nor too small for it. For *E. coli*, the front end entails conversion of glucose to ATP and the back end entails the expenditure of ATP. In short, if the cell invests too heavily in ribosomes, it will not have enough NRPs to catalyze the biochemical conversion of glucose to ATP. The optimization of energy efficiency for fast-replicating cells occurs within the maximal growth rate, which corresponds to a matching of the catabolic and anabolic fluxes

$$\lambda^\infty = k_r f_r^\infty = \lambda_a f_p^\infty, \qquad \textbf{[15]}$$

where λ_a is related to the NRP's rate constant for energy generation (*SI Text*).[¶]

This argument can also be framed in terms of energy costs. Making ribosomes is more expensive than making NRPs per unit weight. The evolutionary tradeoff is between the intrinsic cost of energy-expensive ribosomes needed for fast growth, on the one hand, and the unavoidable cost of NRP turnover at slow growth. As a caveat, to be clear, we note that our efficiency quantity describes the conversion of ATP, not glucose, to proteins and ribosomes. Therefore, our arguments about optimizing energy efficiency do not address the relative importance of fermentation to respiration. Also, the energy optimization described here pertains to evolutionary timescales, over which cells can alter their machine constants. Stressing cells can certainly lead to nonoptimality under daily growth conditions, in ways that could only be improved by evolutionary changes.

[§]We take their values to be $\varepsilon_{rp} = (\varepsilon_p - \varepsilon_r)/\varepsilon_r = 1$, which is a stoichiometric ratio; $\gamma = 0.1$ 1/h, which is the protein degradation rate fixed by protein hydrolysis chemistry; and $k_p' = 9.7$ 1/h, which is the *E. coli* translation speed (alternatively expressed as 20 amino acids per second; Table 1).

[¶]λ_a is the ratio of a cell's total ATP generation flux to the ATP cost of making 1 NRP molecule; it has units of hours^{-1} and represents a driver of biomass growth. It has an impression of efficiency of the metabolic proteins for energy production and could also be measured from experiments.

Table 2. Parameters of *E. coli* ODE numerical model obtained from fit of the model to data

ODE model parameters	Symbol	Value
Affinity constant between NRPs and glucose for glucose transport	D_g	0.07 mM
Number of glucose molecules metabolized to ATP per hour per protein molecule	k_a^∞	120 h^{-1}
Affinity constant between proteins and ATP for ATP generation	D_a	4.0 mM
ATP concentration threshold for ribosome synthesis	D_r	0.18 mM
Maximum fraction of ribosomes translating RPs	f_r^∞	0.2
Maximum fraction of ribosomes translating NRPs	f_p^∞	0.7

The Cell Shifts Its Energy Flows Under Different Growth Conditions

What are the cellular activities under different growth conditions? Fig. 4 gives a summary of the model results. First, under slow-growth conditions, the cell is not efficient at converting energy to proteins or ribosomes (Fig. 4A). Under slow growth, the cell invests its energy in maintenance, replenishing proteins that are degrading.$^{\|}$ The blue dashed curve shows that the efficiency would be much higher if there were no protein degradation (i.e., $\gamma = 0$). Fig. 4 *F* and *G* shows that the cell is producing mostly NRPs, and Fig. 4*H* shows that most of energy in NRPs is going into protein degradation and not dilution under slow-growth conditions.

Second, at higher glucose levels, growth efficiency increases. Under fast-growth conditions, protein degradation happens at a negligible rate, so less of the cell's energy is devoted to repairing degrading proteins. Now, the cell converts more sugar directly to cell growth. Maximal values of yield of biomass from ATP have been widely estimated before in aerobic *E. coli* grown in glucose and other carbon sources (30, 31); our model is consistent with that data. Third, increasing sugar leads to upshifting the production of ribosomes relative to NRPs (6, 10, 32, 33). Experiments are often used to determine ϕ, the mass fraction of all of the cellular proteins that are ribosomal. Previous work has shown that $\phi(\lambda) \propto \lambda$, i.e., ϕ increases linearly with the growth rate of the cell (10). Here, we show how $\phi(\lambda)$ is related to machine constants of the cell. Using Eq. **8**, we find that ϕ is given by

$$\phi(\lambda; f_p) = \frac{M_r R}{M_r R + M_p P} = \frac{\lambda + \gamma}{\lambda + \gamma + k_p' f_p}, \quad [16]$$

where $k_p' = (M_p k_p / M_r)$ is the speed of protein translation. In *E. coli*, k_p' is a constant of 20 amino acids per second per ribosome at 37 °C (6). We find that**

$$\phi(\lambda) = \phi_0 + \frac{\lambda}{k_p' f_p^\infty}, \quad [17]$$

where $\phi_0 = (\gamma/k_p' f_p^\infty)$. Eq. **17** predicts the observed linear relationship (6, 10) in terms of the physical variables in our model: γ, the protein degradation rate, and f_p^∞, the fraction of ribosomes that are translating NRPs at the speed limit for growth. Also, we noted above that, under the fast-growth limits, ribosomes produce about four mass equivalents of NRPs for every mass

equivalent of RPs. This comes from using $\phi \lesssim f_r^\infty = f_r^{\infty,*} \sim 0.2$, which gives $(RP/NRP) = \phi/(1 - \phi) \sim 1/4$ (Fig. 2A).

Fourth, the model predicts that the net protein elongation rate per ribosome, k_{per}, should increase with the cell's growth rate, consistent with direct measurements of single peptide chain extension rates (34–39) (Fig. 5). The error in prediction is within 20% arising from discounting inactive ribosomal fraction (39). Sometimes called ribosomal efficiency, here its growth rate dependency (14, 40, 41) stems mainly from the synthesis of non-ribosomal proteins against their tendency to turnover, especially at small growth, and also on the demand to make more energy-sensitive ribosomes at increased growth rates. Fig. S2B shows the average time, the inverse of the rate, for extending the NRP chain by one amino acid per ribosomal catalyst. This time varies from 0.65 s under slow growth to 0.15 s at fast growth.

Limitations of the Model

To focus on the essentials, our modeling has neglected certain factors of lesser importance for our purposes. First, the model only treats implicitly, and not explicitly, certain processes such as glucose transport across membrane, transcription of RNA, and translation of ribosomal proteins. These are implicit in quantities
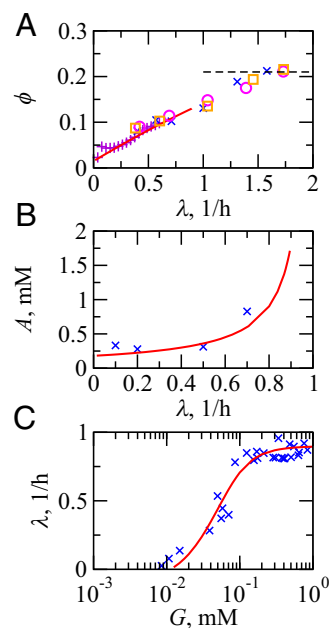
Fig. 2. Comparison of model results (—) vs. experiments (symbols) at 37 °C. (*A*) The RP as a fraction of total protein weight in *E. coli*: °, Bremer and Dennis (6); ×, Scott et al. (10); and □ Forchhammer et al. (44). To get ϕ, the (rRNA/protein) ratio from ref. 10 is scaled by a factor of 0.46 (6). +, fraction of ribosomal promoter activities of Zaslaver et al. (33) uniformly scaled to align with (°, ×, □). At fast growth, ϕ reaches a limit of 0.21 (- - -). (*B*) ATP concentration, *A*, in *E. coli* K-12 strain vs. specific growth rates of cells: ×, Ishii et al. (45). (*C*) *E. coli* specific growth rate vs. extracellular glucose concentration: ×, Monod (1).

$^{\|}$Maintenance energy has been defined in previous works through the use of linear models where the metabolic J_a is often decomposed into a growth and a nongrowth term. The nongrowth term has been called the maintenance energy requirement. These models generally are not valid over the entire range of growth rate from small to large because the maintenance energy is not a constant (42). Here, we treat efficiency without requiring a linearization approximation.

**We consider the fast-growth limit, where $\lambda + \gamma \ll k_p' f_p^\infty$. This condition is not very restrictive, however, because whenever glucose is limiting, *E. coli*'s fastest division time is about 45 min, which is much longer than the timescale of NRP translation per ribosome: $1/(k_p' f_p^\infty) \approx 6.4$ min division time. Also note that a good approximation under fast-growth conditions is $f_p \approx f_p^\infty$ (Fig. S2A).
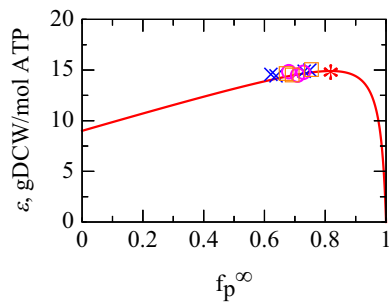
Fig. 3. The fitness landscape of energy efficiency ε vs. f_p^∞—the fractional amount of ribosomes translating NRPs at fast growth. The solid line is Eq. **S18**, grams of cell dry weight (gDCW) per mole of ATP, with machine constants k_p', k_r, and $(\gamma/\varepsilon_{rp})$ from Table 1. * Predicted maximum. The symbols $\bigcirc$, $\times$, and $\square$ show values of f_p (same as Fig. S2A) from experiments across all nutrients and growth rates $\lambda \gtrsim 0.7$ 1/h obtained from Eq. 16 with $\gamma = 0.1$ h^{-1} and $k_p' = 9.7$ h^{-1}, whereas the symbol heights are model-efficiency transformed from $\phi(\lambda)$ data via Eq. **S17**. $\bigcirc$, Bremer and Dennis (6); $\times$, Scott et al. (10); $\square$, Forchhammer et al. (43). The f_p values are consistent with the predicted fitness peak, if the evolutionary target is to maximize the energy efficiency of the fastest-growing cells.

λ_a and k_r. The slowest rate coefficient (under fast growth) is λ_a, which characterizes metabolism and not the production of

Fig. 4. Behaviors of the model cell. (A) Growth efficiency ε (30, 31) (solid blue) and its components ε_p' (solid green) and ε_r' (solid red) (Eq. **S20**); efficiency in the absence of protein turnover $\varepsilon(\gamma = 0)$ (dashed blue). (B) A Lineweaver–Burk plot linearizes the reciprocals of yield ($1/\varepsilon$) and growth rate ($1/\lambda$) from the model. •, experimental maximum biomass yield per unit ATP, $\varepsilon_{max} = 13.9$ gDCW/mol ATP (30). (C–E) How the concentrations of ribosomes (R), NRPs (P), and ATP (A) depend on glucose concentration G. Ribosomal density in units of 10^4 ribosomes/fL is displayed in red and compares well against ref. 46. (F) The flux of ATP into R and P for different growth conditions, G, total ATP generation flux $m_a J_a$ (blue), and ATP consumption fluxes for biosynthesis of ribosomes $m_r J_r$ (red) and NRPs $m_p J_p$ (green) in units of moles per liter per hour (Eq. 10). (G) Predictions of fractional ATP flux toward synthesis of ribosomes $j_r = (m_r J_r)/(m_a J_a)$ (red) and NRPs $j_p = (m_p J_p)/(m_a J_a)$ (green). (H) Fraction of ATP flux used for NRP synthesis split between dilution $(\lambda \cdot P)/J_p$ (dashed green) and degradation $(\lambda \cdot \gamma)/J_p$ (solid green).
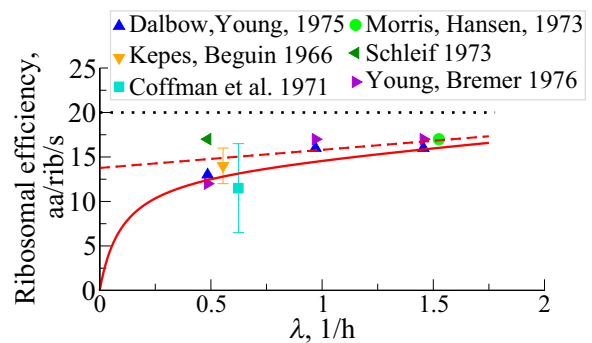

Fig. 5. Net peptide elongation rate, per ribosome, k_{per}, in units of amino acids per second per ribosome vs. cell growth rates, taken over both RPs and NRPs. The solid symbols are direct observations of peptide chain elongation (34–39). The red solid and the dashed lines are predictions with NRP turnover rate $\gamma = 0.1$ h^{-1} and $\gamma = 0$, respectively [Eq. **S14a**; $f_p = f_p^\infty$. (...) indicates maximal translation rate].

protein. With these simplifications, there are energy sources and sinks in the cell that we have not modeled here. Second, we have only considered respiration. It is well known that aerobic *E. coli* uses fermentative metabolism at fast growth rates. In quantitative terms, fermentation contributes increasing energy at faster growth rates. However, the amounts are small. We estimate this contribution to be ~10% at $\lambda = 0.6$ h^{-1}.[††] Interestingly, the cell's optimal energy efficiency state (Eq. **14**) is given by properties unrelated to the mode of energy generation. Third, we considered the efficiency of energy to biomass, a property that is difficult to measure. More experiments for accurate estimates are required. However, based on indirect measurements, it has been suggested that maximal energy efficiency seems to lie close to maximal growth rates (18). Fourth, our model is relevant in the growth speed regime $0.1 \lesssim \lambda \lesssim 1$ h^{-1} as observed in glucose-limited cultures. At slower growth rates, stress machineries and chaperones are activated, whereas at very fast growth, additional nutrient supplements are required, which we do not consider.

Discussion

We developed a coarse-grained model of the concentrations and fluxes of the basic energy and biomass flows in a typical bacterial cell such as *E. coli*. With three dynamical equations and one constraint relationship, taken in the steady-state limit, this is about the simplest model of the energy–biomass balance of a simple cell, which is a complex and nonlinear system. It predicts the fluxes and concentrations of ATP and RPs and NRPs as a function of glucose concentration. The model also gives an expression for the linear law of ribosomal increase with growth rate and how it depends on the cell's machine constants, and it expresses the basic behavior that cells invest energy in repairing proteins when sugar is low vs. duplicating when sugar is high. The model gives a relationship between the cell's growth law and its fitness landscape. It explains why each ribosome in *E. coli* duplicating at full speed produces about four mass equivalents of NRP for every unit mass of RP. The present model shows that the observation can be explained if the evolutionary fitness function for *E. coli* is the energy efficiency of the fast-growing cells instead of the maximum speed itself or some other property. This appears as a result of evolution in which a cell achieves
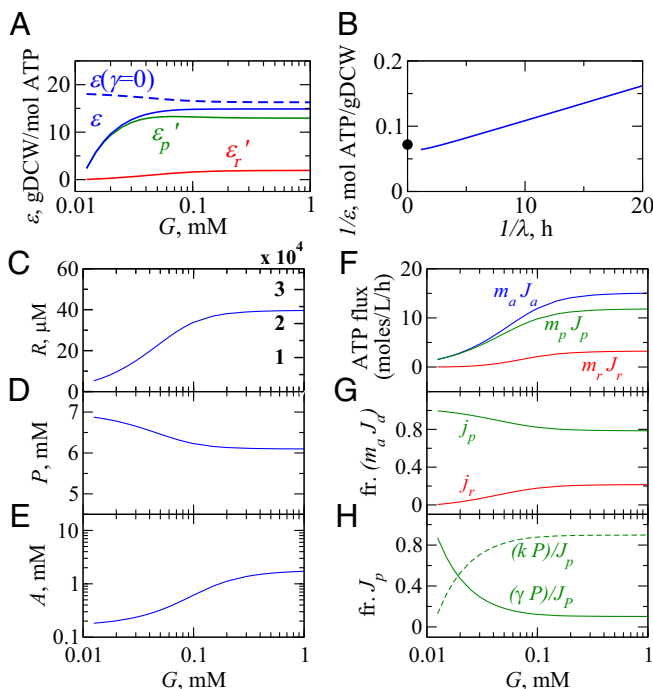

[††]At about $\lambda = 0.6$ 1/h, the glucose uptake flux is ~1.5 g glucose/g dry cell weight per hour, and acetic acid export flux is ~0.4 g acetic acid/g dry cell weight per hour (43). Assuming 50% of the glucose up take produces ATP at 30 ATP per glucose molecule by respiration, whereas fermentation of glucose to acetic acid produces 2 ATP per acetate gives the percentage of ATP generation by fermentation to be about 10%. We consider mol. wt. of glucose and acetate to be 180 and 60 Da, respectively.

a balance between the cost of energy-expensive ribosomes required for fast replication, on the one hand, and the unavoidable costs of maintaining proteins against instability, denaturation, and turnover, on the other hand, which are important under slow-growth conditions.

1. Monod J (1949) The growth of bacterial cultures. *Annu Rev Microbiol* 3:371–394.
2. Hinshelwood CN (1952) On the chemical kinetics of autosynthetic systems. *J Chem Soc* 745–755.
3. Ehrenberg M, Kurland CG (1984) Costs of accuracy determined by a maximal growth rate constraint. *Q Rev Biophys* 17(1):45–82.
4. Koch AL (1988) Why can't a cell grow infinitely fast? *Can J Microbiol* 34(4):421–426.
5. Cox RA (2004) Quantitative relationships for specific growth rates and macromolecular compositions of Mycobacterium tuberculosis, Streptomyces coelicolor A3(2) and Escherichia coli B/r: An integrative theoretical approach. *Microbiology* 150(Pt 5): 1413–1426.
6. Bremer H, Dennis P (1996) Modulation of chemical composition and other parameters of the cell by growth rate. *Escherichia coli and Salmonella*, ed Neidhardt FC (American Society for Microbiology Press, Washington, DC).
7. Phillips R, Milo R (2009) A feeling for the numbers in biology. *Proc Natl Acad Sci USA* 106(51):21465–21471.
8. Youk H, van Oudenaarden A (2009) Growth landscape formed by perception and import of glucose in yeast. *Nature* 462(7275):875–879.
9. Klumpp S, Zhang Z, Hwa T (2009) Growth rate-dependent global effects on gene expression in bacteria. *Cell* 139(7):1366–1375.
10. Scott M, Gunderson CW, Mateescu EM, Zhang Z, Hwa T (2010) Interdependence of cell growth and gene expression: Origins and consequences. *Science* 330(6007):1099–1102.
11. Scott M, Hwa T (2011) Bacterial growth laws and their applications. *Curr Opin Biotechnol* 22(4):559–565.
12. Scott M, Klumpp S, Mateescu EM, Hwa T (2014) Emergence of robust growth laws from optimal regulation of ribosome synthesis. *Mol Syst Biol* 10:747.
13. Orr HA (2009) Fitness and its role in evolutionary genetics. *Nat Rev Genet* 10(8): 531–539.
14. Klumpp S, Scott M, Pedersen S, Hwa T (2013) Molecular crowding limits translation and cell growth. *Proc Natl Acad Sci USA* 110(42):16754–16759.
15. Molenaar D, van Berlo R, de Ridder D, Teusink B (2009) Shifts in growth strategies reflect tradeoffs in cellular economics. *Mol Syst Biol* 5:323.
16. Neidhardt F, Ingraham J, Schaechter M (1990) *Physiology of the Bacterial Cell* (Sinauer Associates, Sunderland, MA).
17. Stouthamer AH, Bettenhaussen C (1973) Utilization of energy for growth and maintenance in continuous and batch cultures of microorganisms: A reevaluation of the method for the determination of ATP production by measuring molar growth yields. *Biochimica et Biophysica Acta - Reviews on Bioenergetics* 301(1):53–70.
18. Tempest DW, Neijssel OM (1984) The status of YATP and maintenance energy as biologically interpretable phenomena. *Annu Rev Microbiol* 38:459–486.
19. Dekel E, Alon U (2005) Optimality and evolutionary tuning of the expression level of a protein. *Nature* 436(7050):588–592.
20. Stoebel DM, Dean AM, Dykhuizen DE (2008) The cost of expression of Escherichia coli lac operon proteins is in the process, not in the products. *Genetics* 178(3):1653–1660.
21. Trötschel C, Albaum SP, Poetsch A (2013) Proteome turnover in bacteria: Current status for Corynebacterium glutamicum and related bacteria. *Microb Biotechnol* 6(6):708–719.
22. Dressaire C, et al. (2009) Transcriptome and proteome exploration to model translation efficiency and protein stability in Lactococcus lactis. *PLOS Comput Biol* 5(12): e1000606.
23. Belle A, Tanay A, Bitincka L, Shamir R, O'Shea EK (2006) Quantification of protein half-lives in the budding yeast proteome. *Proc Natl Acad Sci USA* 103(35):13004–13009.
24. Eden E, et al. (2011) Proteome half-life dynamics in living human cells. *Science* 331(6018): 764–768.
25. Zundel MA, Basturea GN, Deutscher MP (2009) Initiation of ribosome degradation during starvation in Escherichia coli. *RNA* 15(5):977–983.
26. Jewett MC, Miller ML, Chen Y, Swartz JR (2009) Continued protein synthesis at low [ATP] and [GTP] enables cell adaptation during energy limitation. *J Bacteriol* 191(3):1083–1091.
27. Westerhoff HV, Hellingwerf KJ, Van Dam K (1983) Thermodynamic efficiency of microbial growth is low but optimal for maximal growth rate. *Proc Natl Acad Sci USA* 80(1):305–309.
28. Schuetz R, Zamboni N, Zampieri M, Heinemann M, Sauer U (2012) Multidimensional optimality of microbial metabolism. *Science* 336(6081):601–604.
29. DeLong JP, Okie JG, Moses ME, Sibly RM, Brown JH (2010) Shifts in metabolic scaling, production, and efficiency across major evolutionary transitions of life. *Proc Natl Acad Sci USA* 107(29):12941–12945.
30. Farmer IS, Jones CW (1976) The energetics of Escherichia coli during aerobic growth in continuous culture. *Eur J Biochem* 67(1):115–122.
31. Kayser A, Weber J, Hecht V, Rinas U (2005) Metabolic flux analysis of Escherichia coli in glucose-limited continuous culture. I. Growth-rate-dependent metabolic efficiency at steady state. *Microbiology* 151(Pt 3):693–706.
32. Schaechter M, Maaloe O, Kjeldgaard NO (1958) Dependency on medium and temperature of cell size and chemical composition during balanced grown of Salmonella typhimurium. *J Gen Microbiol* 19(3):592–606.
33. Zaslaver A, et al. (2009) Invariant distribution of promoter activities in Escherichia coli. *PLOS Comput Biol* 5(10):e1000545.
34. Dalbow DG, Young R (1975) Synthesis time of β-galactosidase in Escherichia coli B/r as a function of growth rate. *Biochem J* 150(1):13–20.
35. Kepes A, Beguin S (1966) Peptide chain initiation and growth in the induced synthesis of beta-galactosidase. *Biochim Biophys Acta* 123(3):546–560.
36. Coffman RL, Norris TE, Koch AL (1971) Chain elongation rate of messenger and polypeptides in slowly growing Escherichia coli. *J Mol Biol* 60(1):1–19.
37. Morris DR, Hansen MT (1973) Influence of polyamine limitation on the chain growth rates of beta-galactosidase and of its messenger ribonucleic acid. *J Bacteriol* 116(2):588–592.
38. Schleif R, Hess W, Finkelstein S, Ellis D (1973) Induction kinetics of the L-arabinose operon of Escherichia coli. *J Bacteriol* 115(1):9–14.
39. Young R, Bremer H (1976) Polypeptide-chain-elongation rate in Escherichia coli B/r as a function of growth rate. *Biochem J* 160(2):185–194.
40. Koch AL (1980) The inefficiency of ribosomes functioning in Escherichia coli growing at moderate rates. *J Gen Microbiol* 116(1):165–171.
41. Pedersen S (1984) Escherichia coli ribosomes translate in vivo with variable rate. *EMBO J* 3(12):2895–2898.
42. Neijssel O, de Mattos MT, Tempest D (1996) Growth yield and energy distribution. *Escherichia coli and Salmonella*, ed Neidhardt FC (ASM Press, Washington, DC).
43. Vemuri GN, Altman E, Sangurdekar DP, Khodursky AB, Eiteman MA (2006) Overflow metabolism in Escherichia coli during steady-state growth: transcriptional regulation and effect of the redox ratio. *Appl Environ Microbiol* 72(5):3653–3661.
44. Forchhammer J, Lindahl L (1971) Growth rate of polypeptide chains as a function of the cell growth rate in a mutant of Escherichia coli 15. *J Mol Biol* 55(3):563–568.
45. Ishii N, et al. (2006) Multiple high-throughput analyses moniter the response of the E. coli to perturbations. *Science* 316(5824):593–597.
46. Bakshi S, Siryaporn A, Goulian M, Weisshaar JC (2012) Superresolution imaging of ribosomes and RNA polymerase in live Escherichia coli cells. *Mol Microbiol* 85(1):21–38.
47. Zhang J (2000) Protein-length distributions for the three domains of life. *Trends Genet* 16(3):107–109.

BIOPHYSICS AND
COMPUTATIONAL BIOLOGY